Electronic Supplementary Material (ESI) for Journal of Materials Chemistry C.

SUPPORTING INFORMAITON

[3 + 3] Imine and β-Ketoenamine Tethered Fluorescent Covalent-Organic Frameworks for CO_2 Uptake and Nitroaromatic Sensing

D. Kaleeswaran‡, Pratap Vishnoi‡, and Ramaswamy Murugavel*

Department of Chemistry, Indian Institute of Technology Bombay, Mumbai, India-400 076.
E-mail: rmv@chem.iitb.ac.in
Tel: +91 22 2576 7163

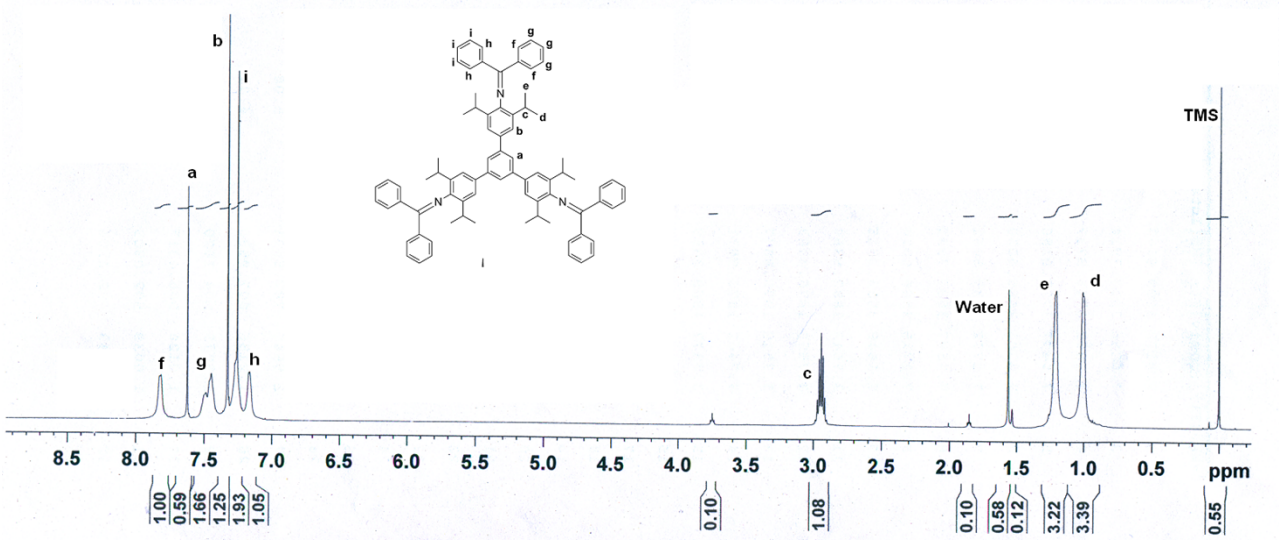

Figure S1. ^{1}H NMR spectrum of *i*PrTAPB-NPh_2 in $CDCl_3$.

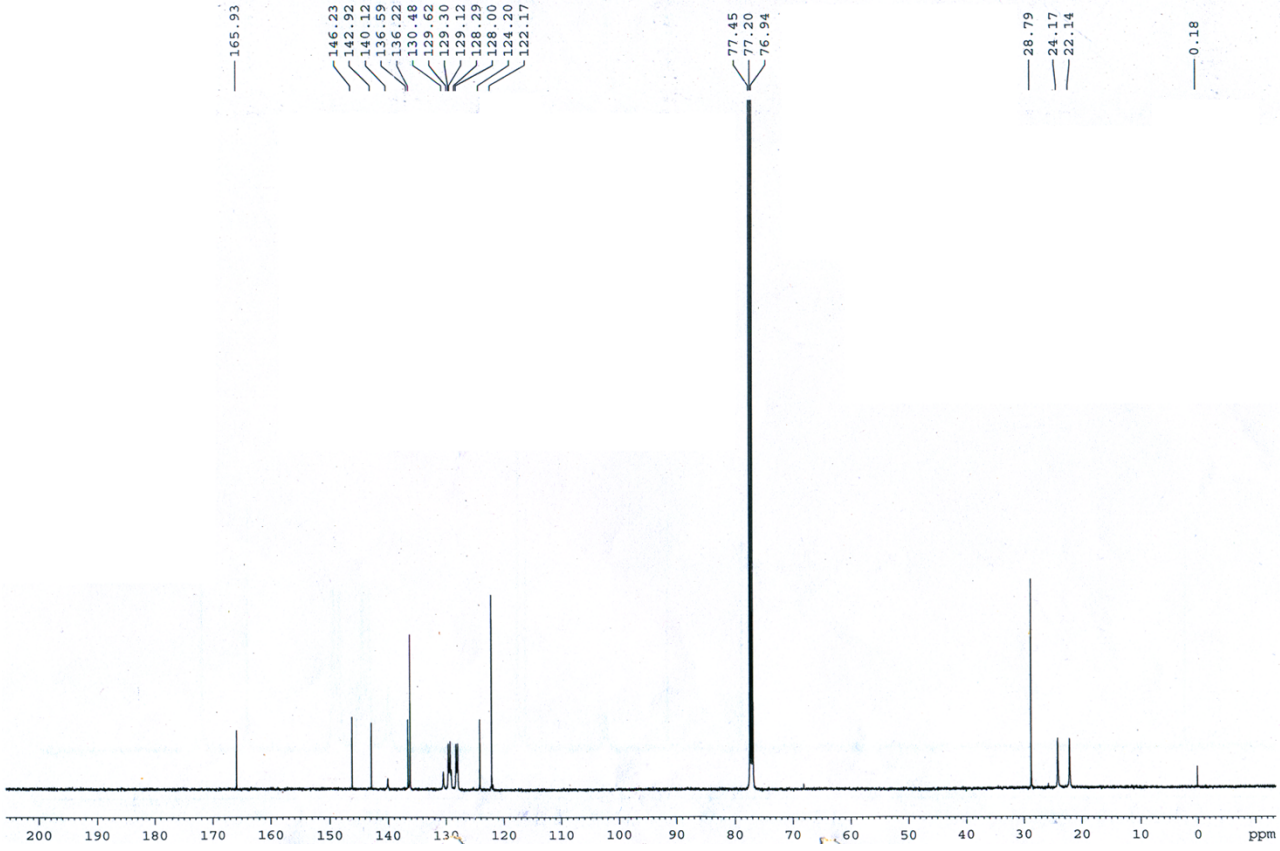

Figure S2. ^{13}C NMR spectrum of *i*PrTAPB-NPh_2 in $CDCl_3$.

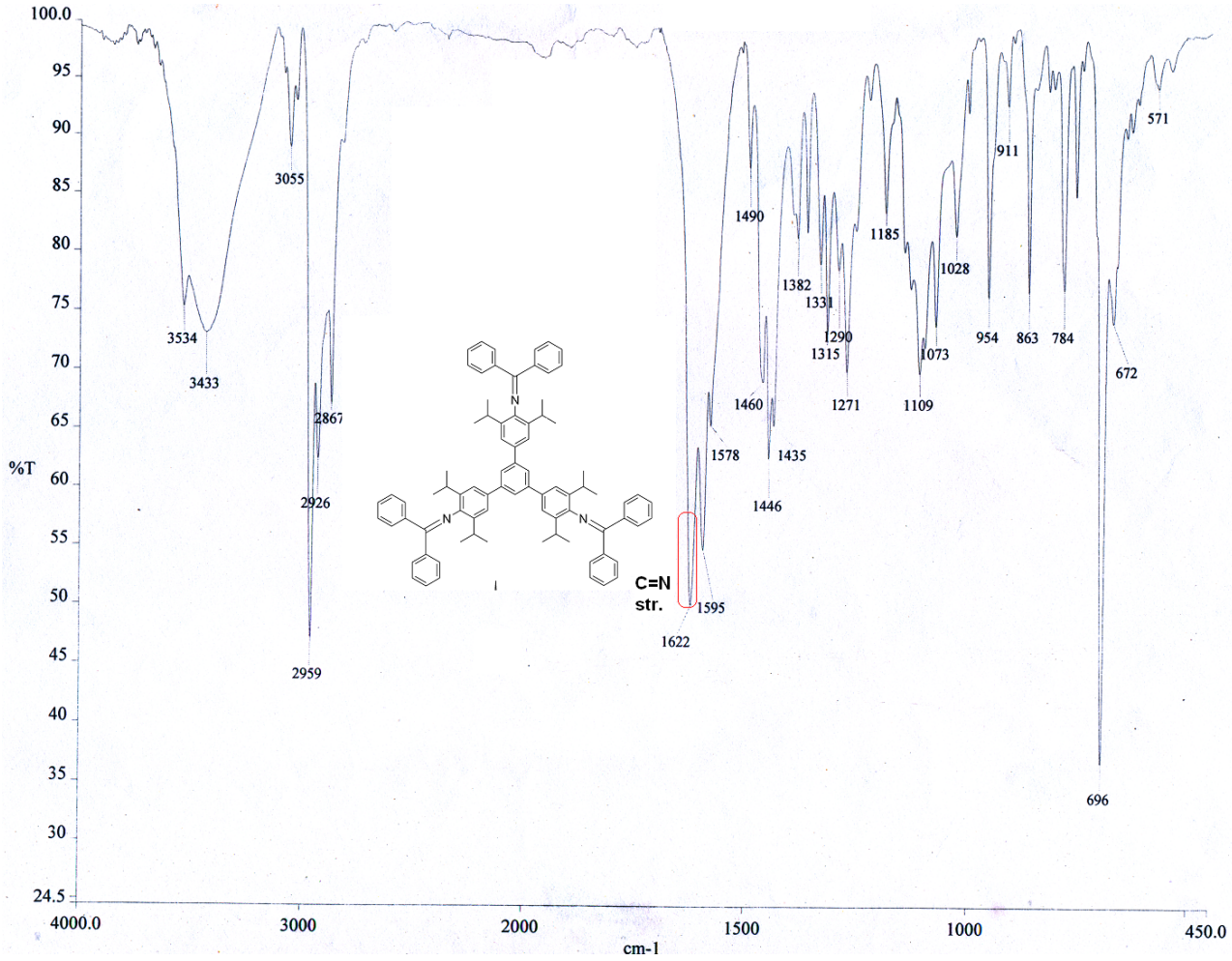

Figure S3. FT-IR spectrum of *i*PrTAPB-NPh_2. (KBr disc).

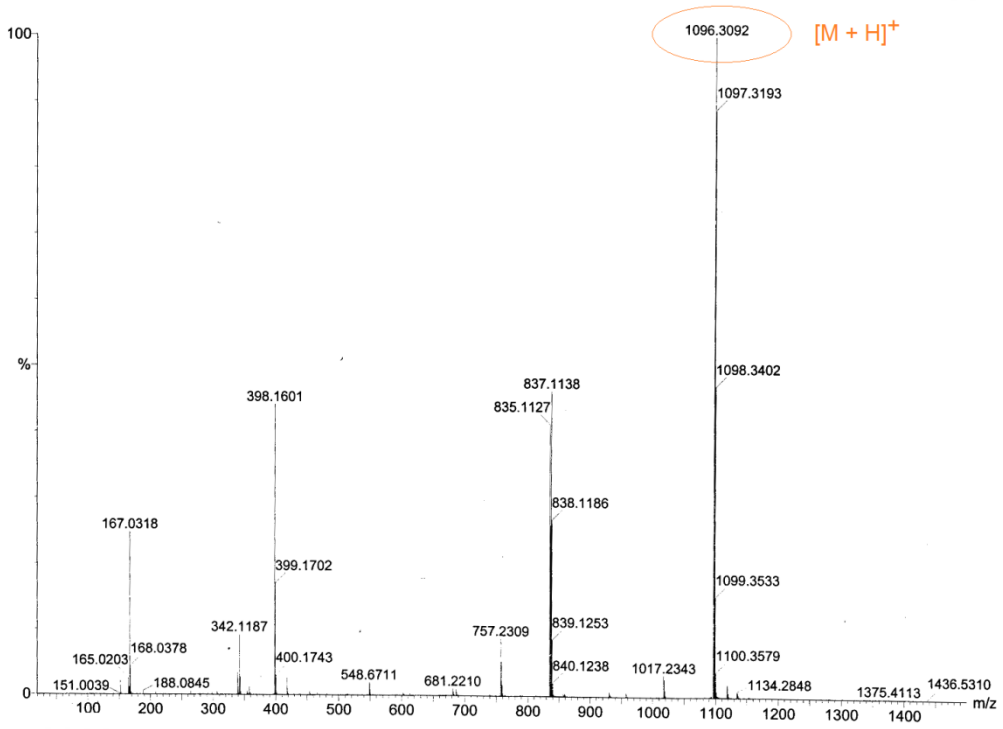

Figure S4. ESI-MS spectrum of *i*PrTAPB-NPh_2.

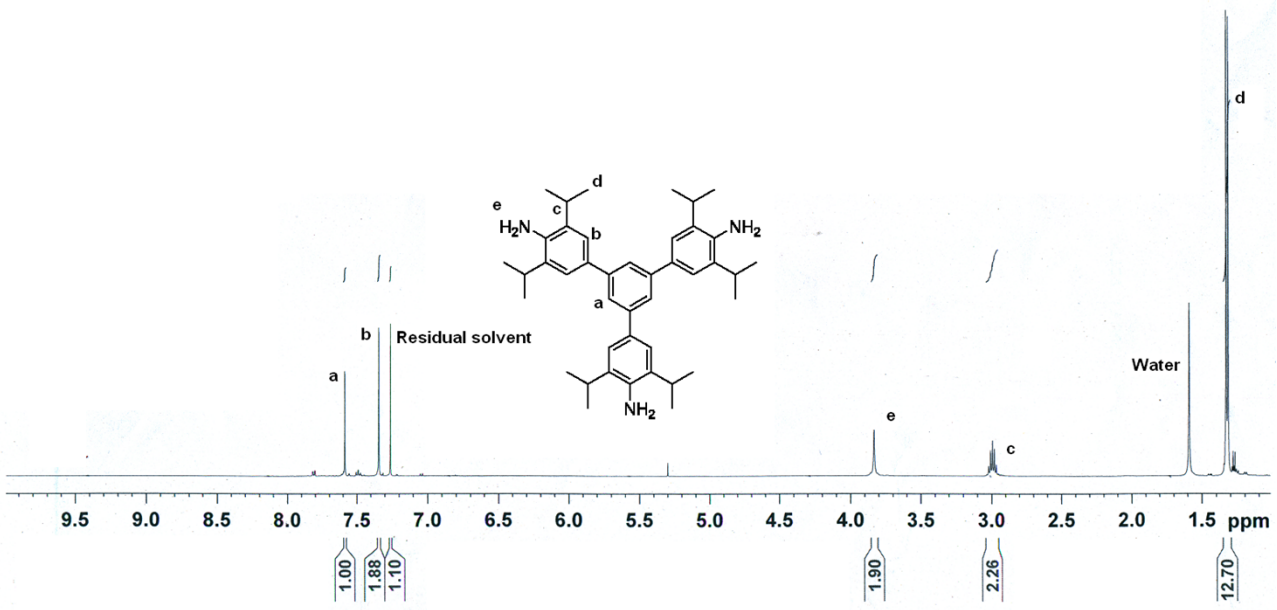

Figure S5. ^{1}H NMR spectrum of *i*PrTAPB in $CDCl_3$.

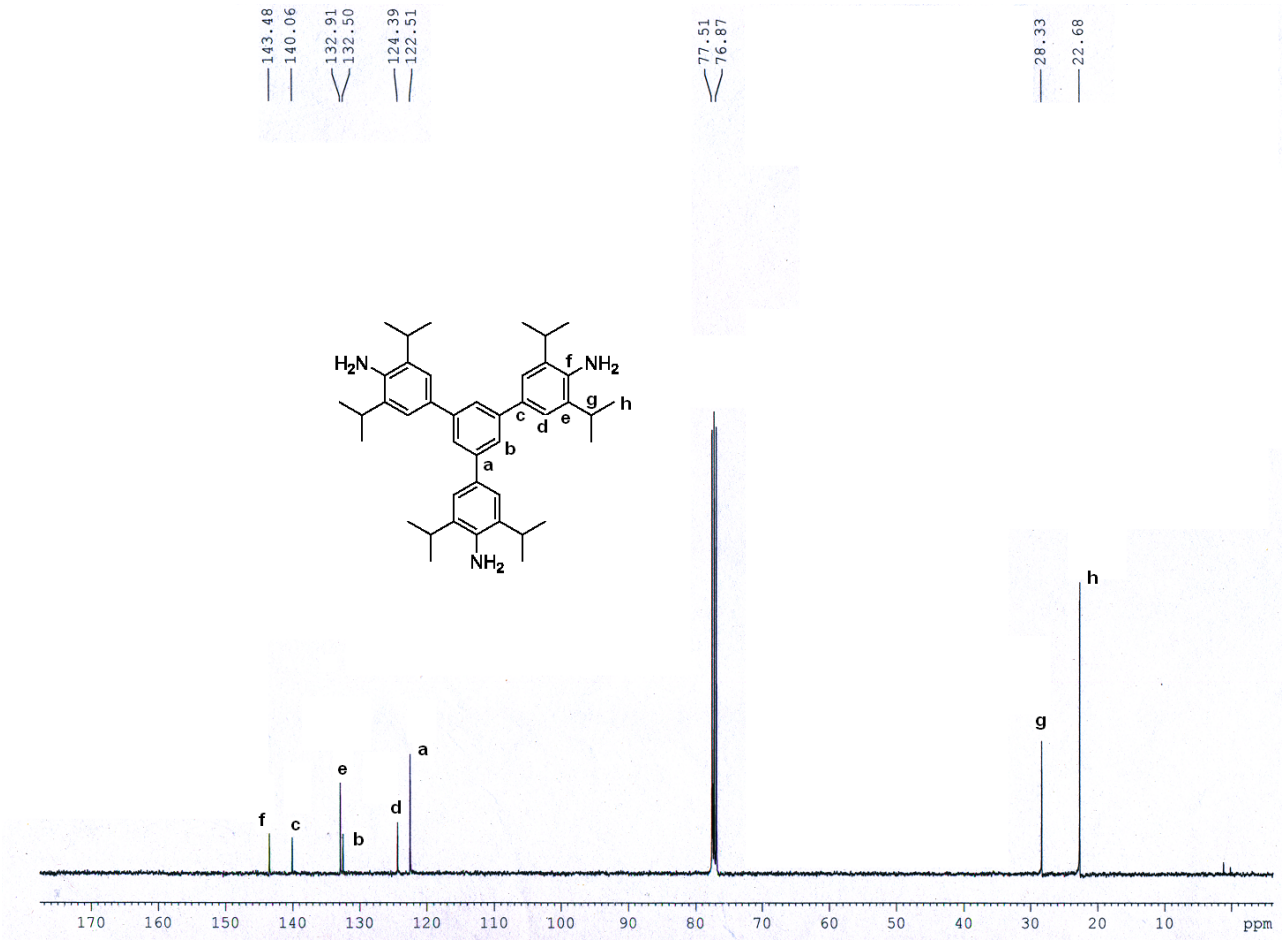

Figure S6. ^{13}C NMR spectrum of *i*PrTAPB in $CDCl_3$.

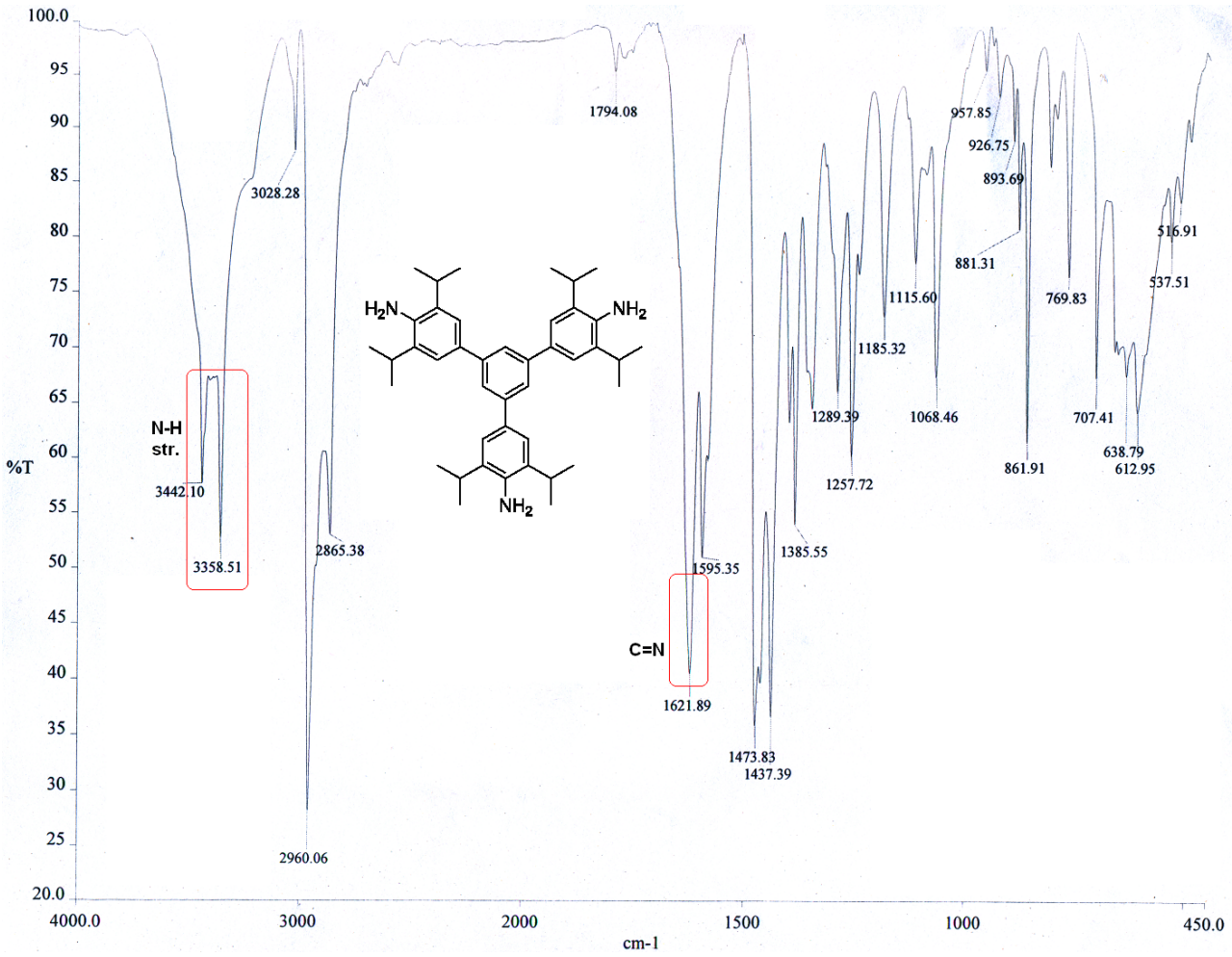

Figure S7. FT-IR spectrum of *i*PrTAPB (KBr disc).

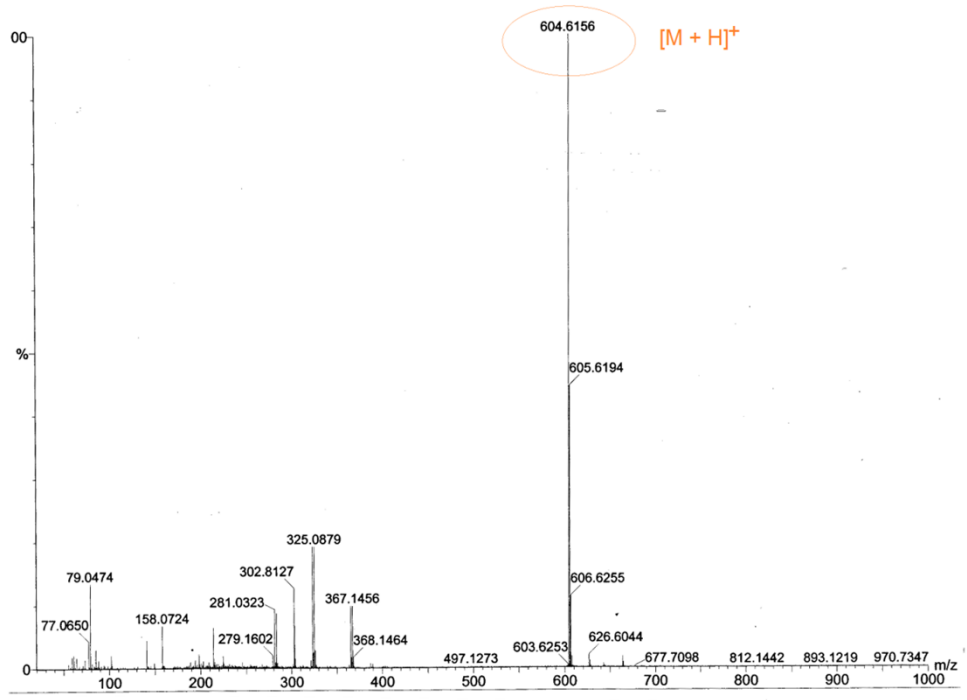

Figure S8. ESI-MS spectrum of *i*PrTAPB.

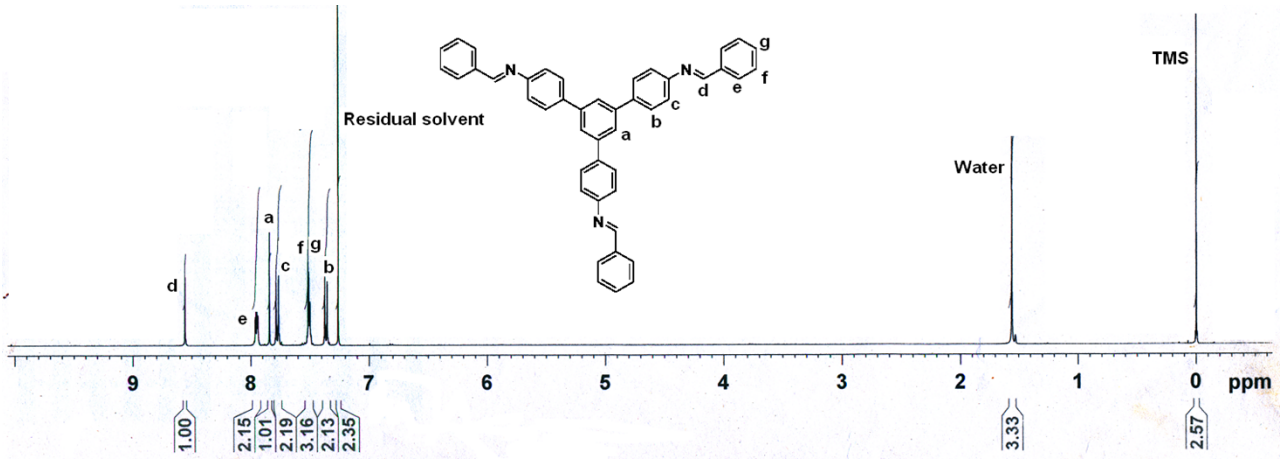

Figure S9. ^{1}H NMR spectrum of TAPB-Benz in $CDCl_3$.

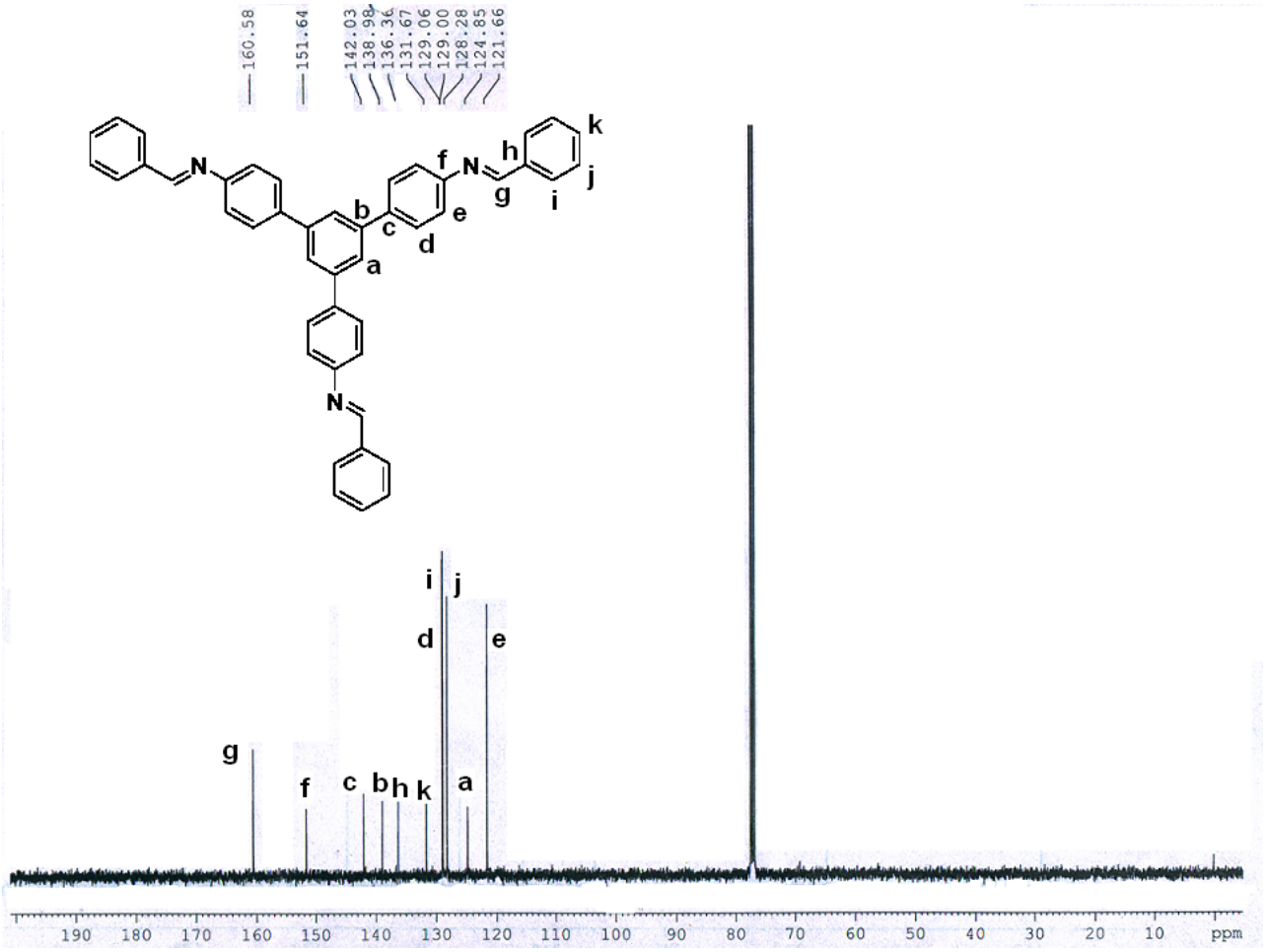

Figure S10. ^{13}C NMR spectrum of TAPB-Benz in $CDCl_3$.

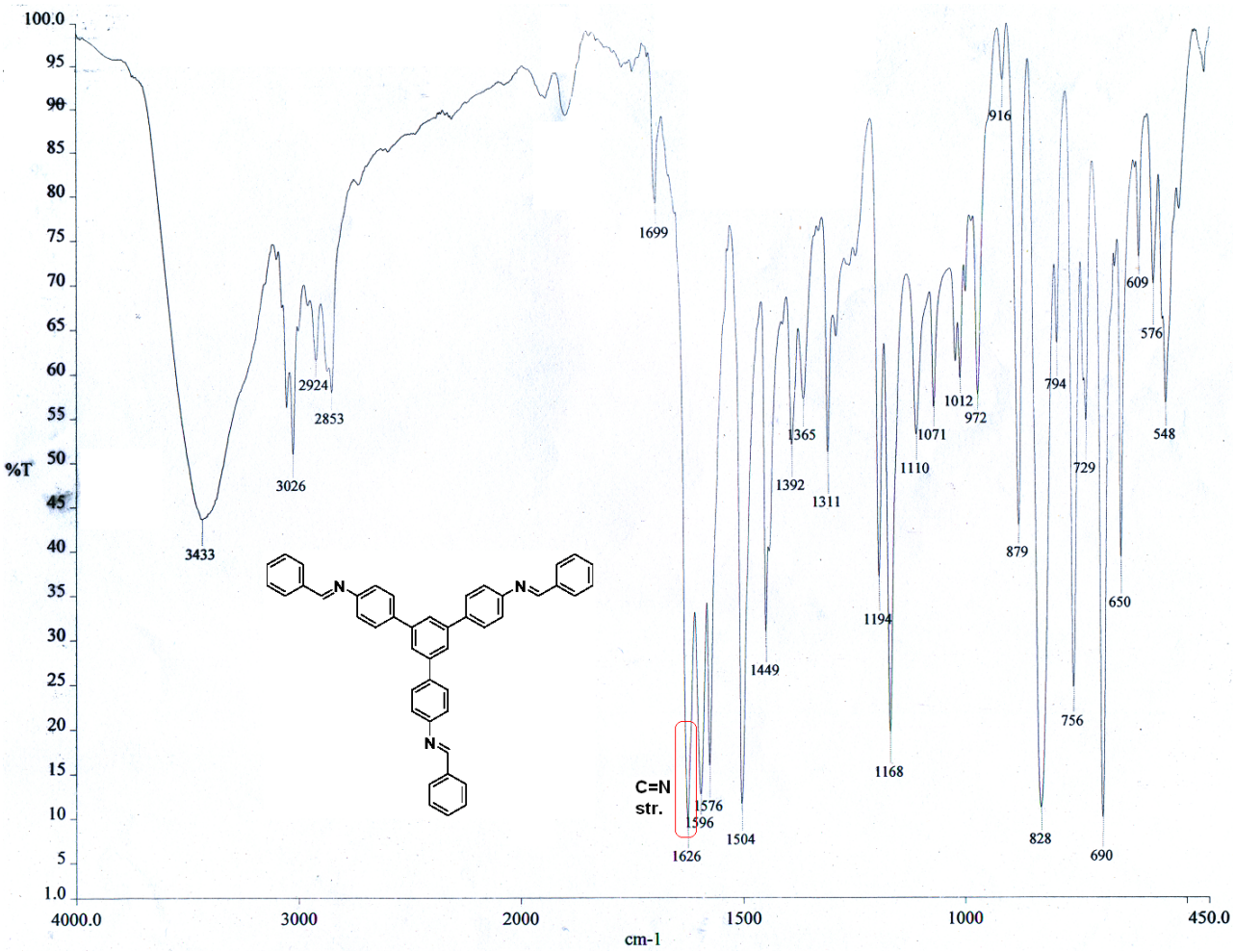

Figure S11. FT-IR spectrum of TAPB-Benz (KBr disc).

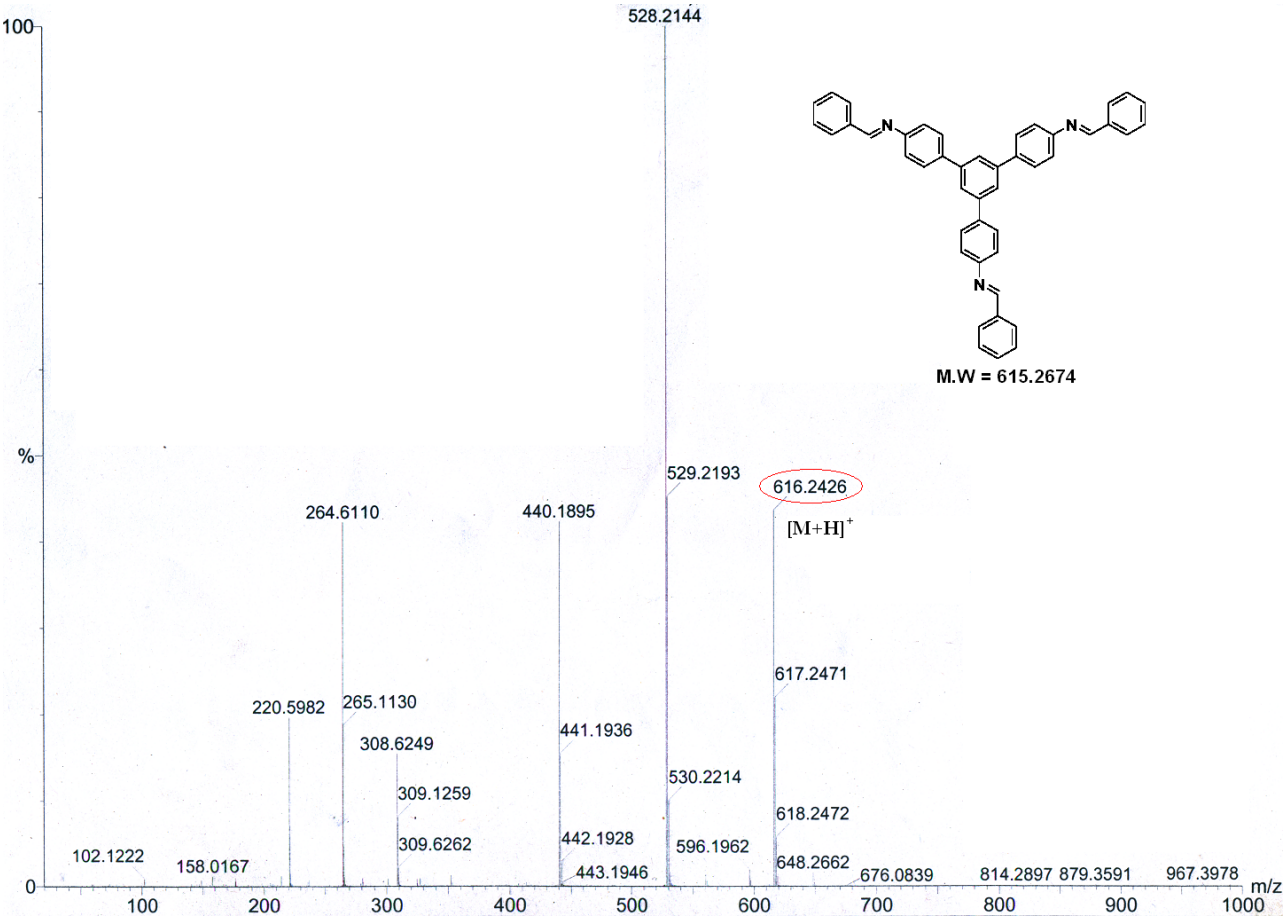

Figure S12. ESI-MS spectrum of TAPB-Benz.

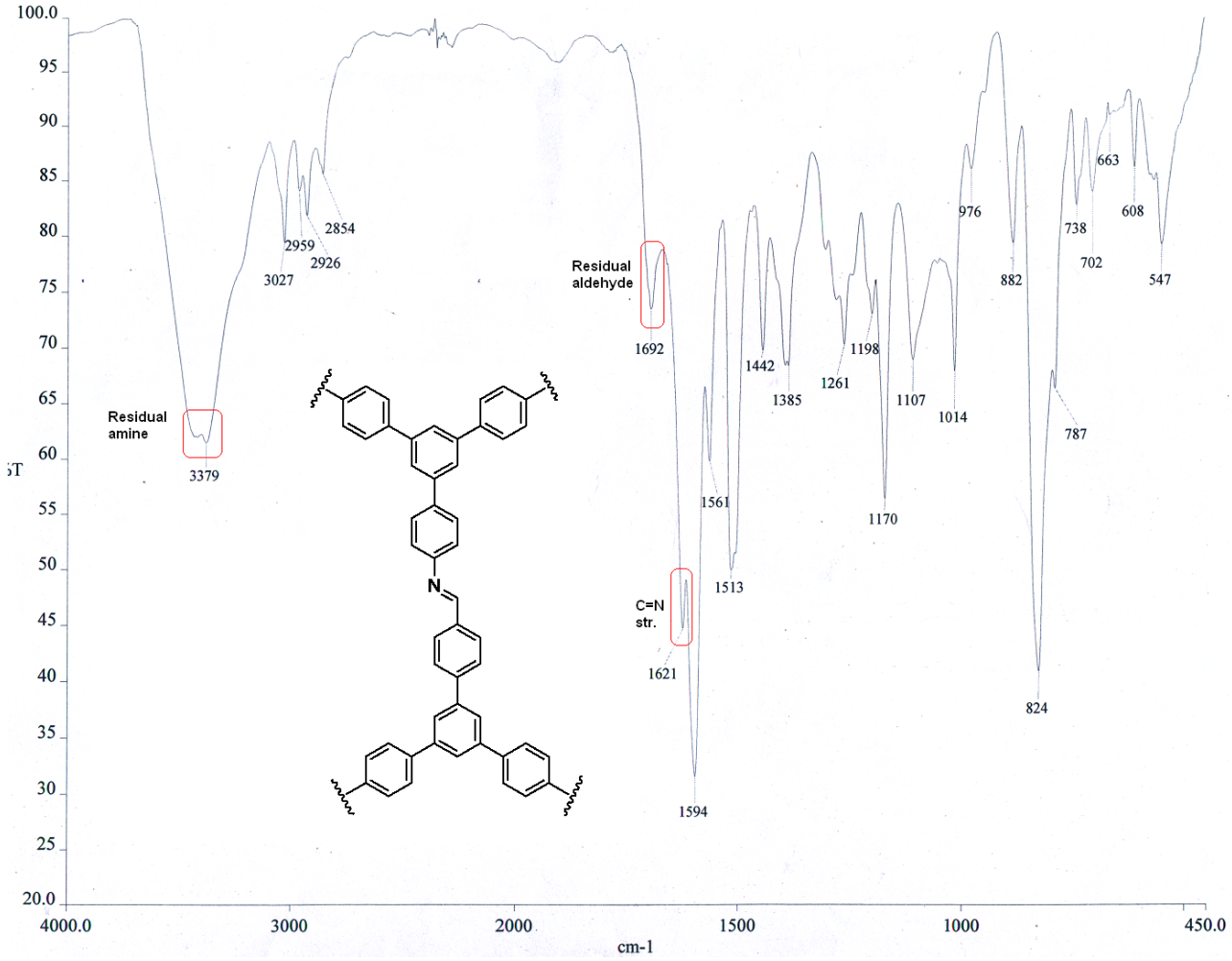

Figure S13. FT-IR spectrum of TAPB-TFPB (KBr disc).

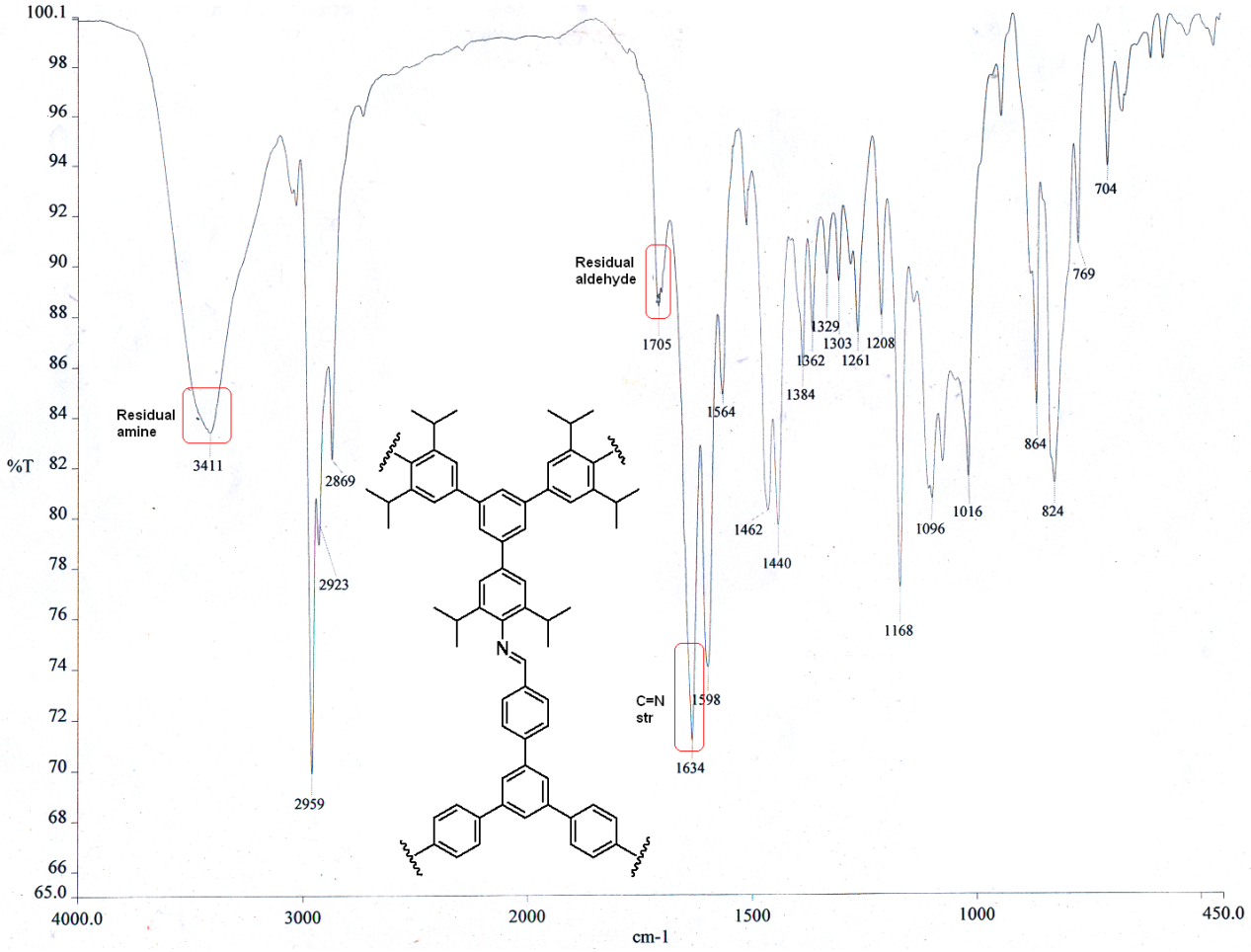

Figure S14. FT-IR spectrum of *i*PrTAPB-TFPB (KBr disc).

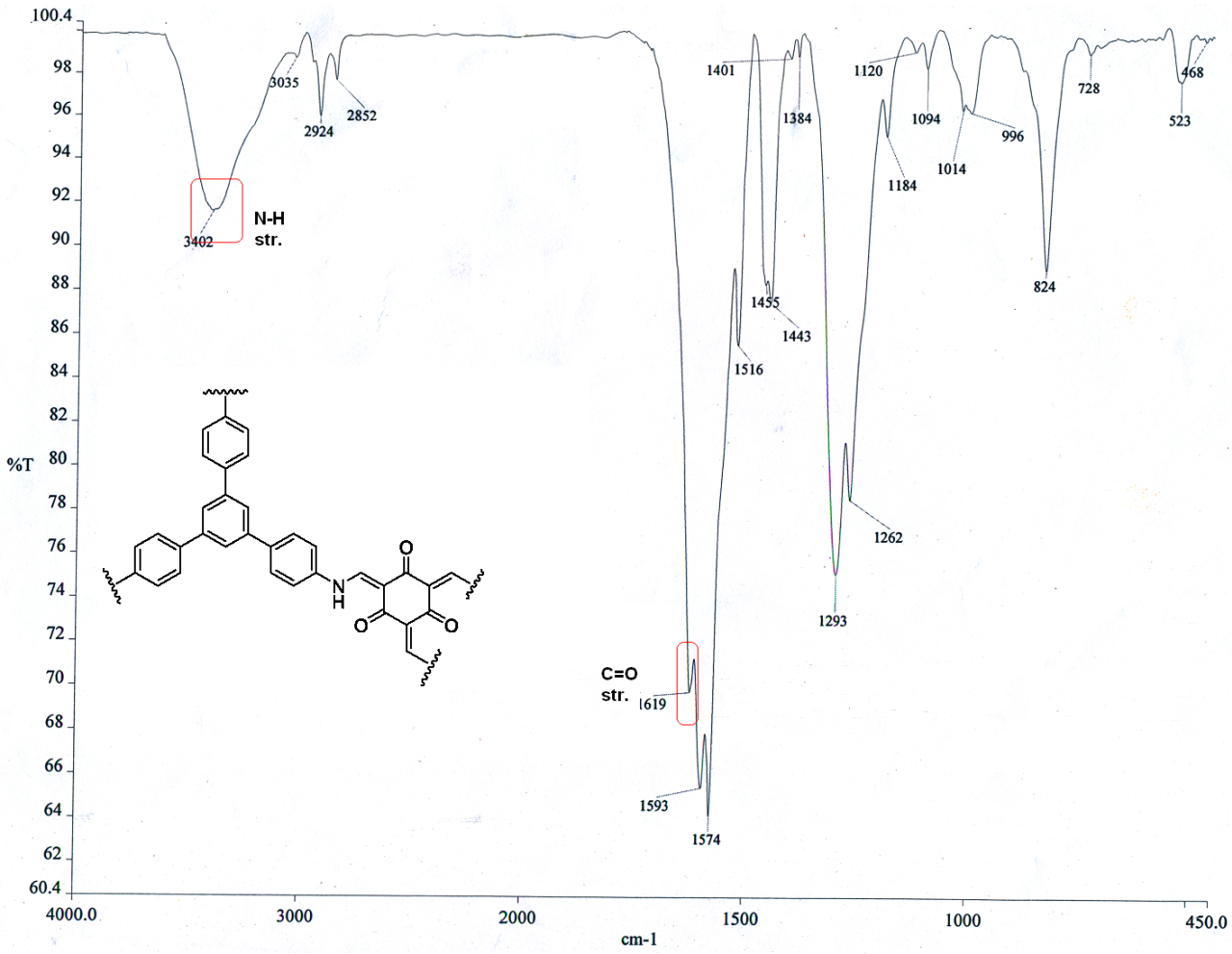

Figure S15. FT-IR spectrum of TAPB-TFP (KBr disc).

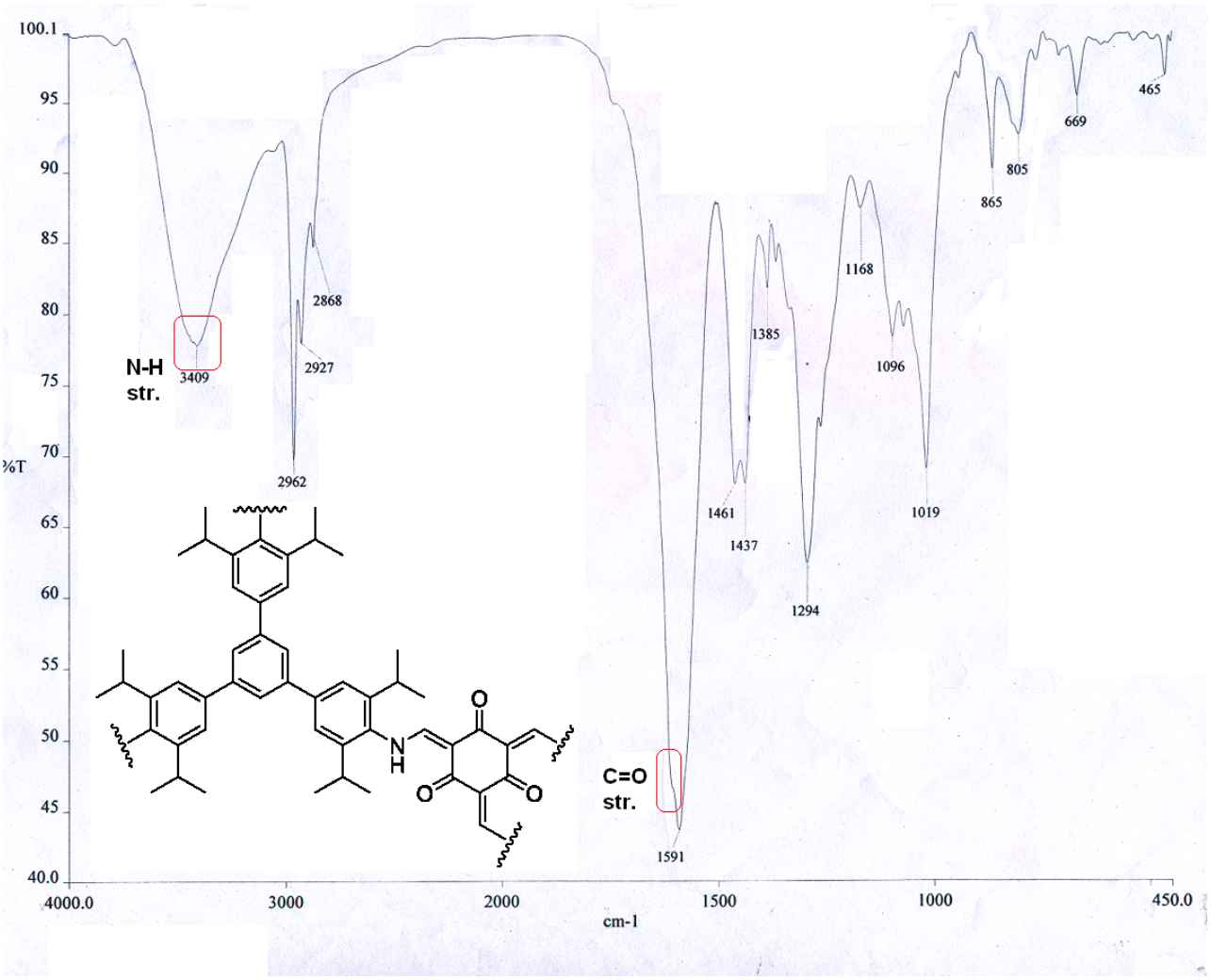

Figure S16. FT-IR spectrum of *i*PrTAPB-TFP (KBr disc).

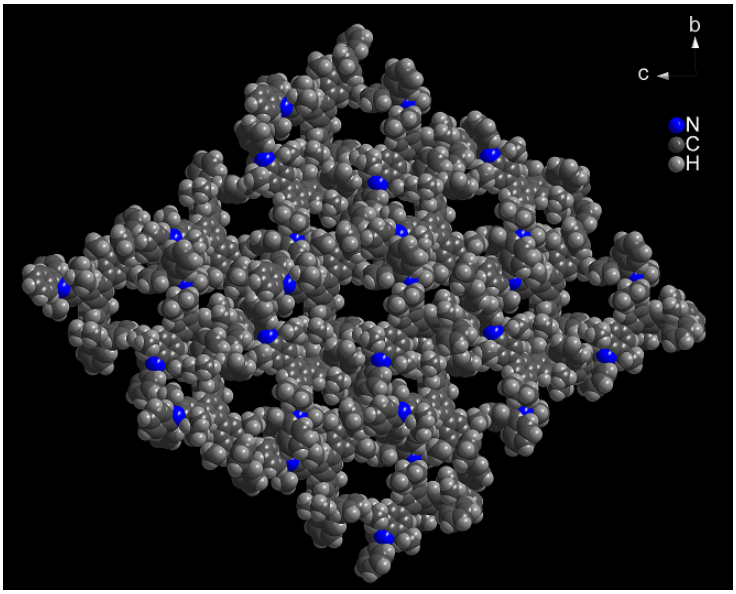

Figure S17. Packing diagram of crystal structure of *i*PrTAPB based on Van der Waals radii of atoms.

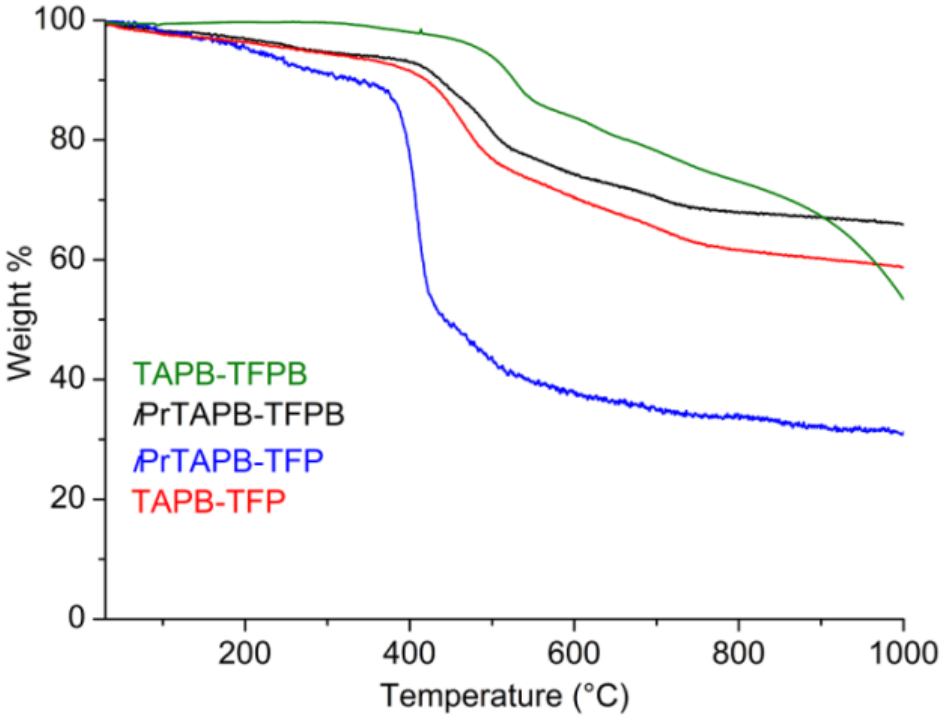

Figure S18. TGA profiles of TAPB-TFPB,TAPB-TFP, *i*PrTAPB-TFPB and *i*PrTAPB-TFP (N_2 atm, 10 °C/min).

Table S1. Comparison of CO_2 uptake at 273 K and 1 bar

Compounds	CO_2 uptake (cc/g)	CO_2 uptake (mmol/g)	CO_2 uptake (mg/g)	CO_2 uptake (wt %)	Reference
TAPB-TFP	91.6	4.09	180	18.0	This work
*i*PrTAPB-TFP	53.5	2.39	105.2	10.52	This work
BFCMP-2	62.0	2.77	122	12.2	1
PBILP	61.8	2.76	121	12.1	2
BILP-10	90.0	4.02	177	17.7	3
BILP-11	69.2	3.09	136	13.6	3
BILP-13	57.5	2.57	113	11.3	3
TB-MOP	86.0	3.84	169	16.9	4
TB-MOP-Ru	64.5	2.88	127	12.7	4
Azo-POF-1	66.7	2.98	131	13.1	5
COP-93	71.2	3.18	140	14.0	6
BILP-5	65.0	2.9	128	12.8	7
TBILP-1	59.4	2.65	117	11.7	8
TCMP-0	53.3	2.38	105	10.5	9
PCTF-1	73.7	3.29	145	14.5	10
TPI-1	54.4	2.43	107	10.7	11
PPF-1	135.7	6.06	267	26.7	11
PPF-2	124.1	5.54	244	24.4	11
PPF-4	58.0	2.59	114	11.4	12
TpPa-1	78.0	3.48	153.1	15.3	13
TpPa-2	64.0	2.85	125.4	12.5	13
PPTBC	65.6	2.93	128.9	12.9	14

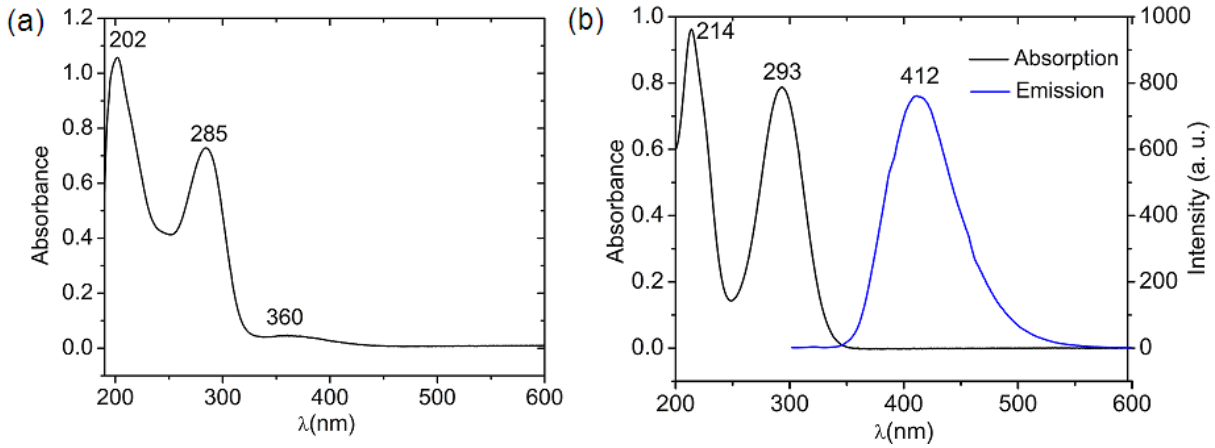

Figure S19. UV-Vis and emission spectra of *i*PrTAPB-NPh_2 and *i*PrTAPB, (a) UV-Vis spectrum of compound *i*PrTAPB-NPh_2 in acetonitrile (8.0 μM); λ_{max} = 202 (ε = 1.32 × 10^5 M cm^{-1}), 285 (ε = 9 × 10^4 M cm^{-1}), 360 (ε = 5 × 10^3 M cm^{-1}) nm; (b) UV-Vis spectrum of compound *i*PrTAPB in acetonitrile (10 μM); λ_{max} = 214 (ε = 9.6 × 10^4 M cm^{-1}), 293 (ε = 7.8 × 10^4 M cm^{-1}), and emission spectrum of *i*PrTAPB in acetonitrile (4.0 μM); λ_{ex} = 293 nm.

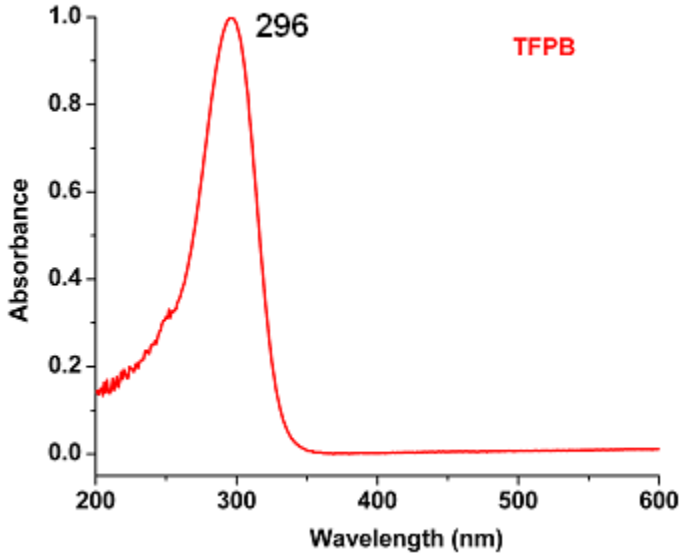

Figure S20. Normalized UV-vis spectrum of TFPB acetonitrile suspension.

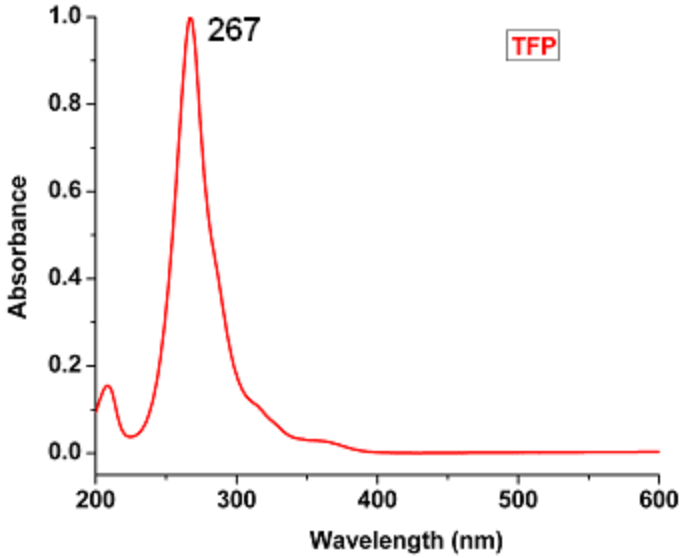

Figure S21. Normalized UV-vis spectrum of TFP acetonitrile solution (1×10^{-5} M).

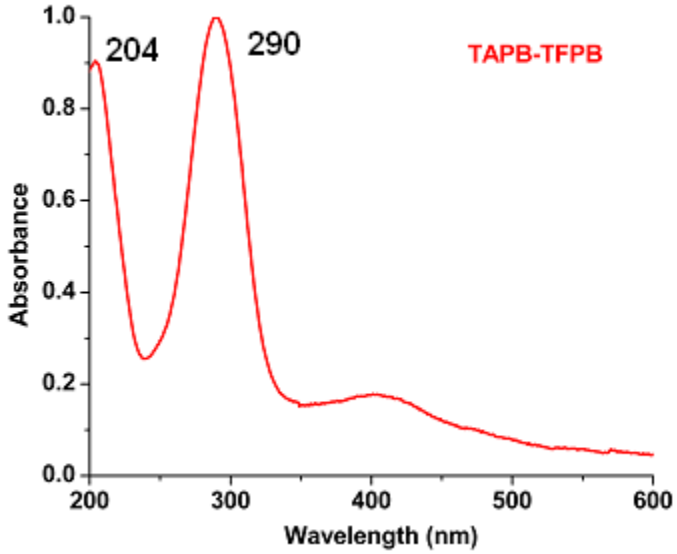

Figure S22. Normalized UV-vis spectrum of TAPB-TFPB acetonitrile suspension.

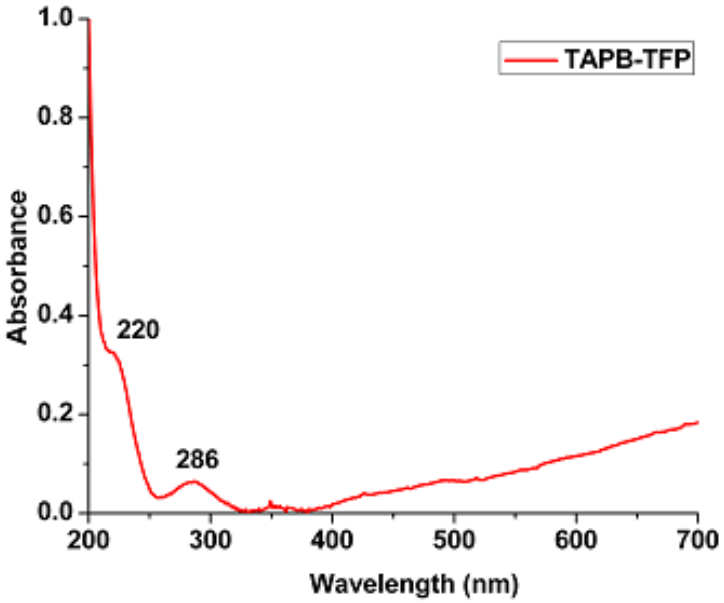

Figure S23. Normalized UV-vis spectrum of TAPB-TFP acetonitrile suspension.

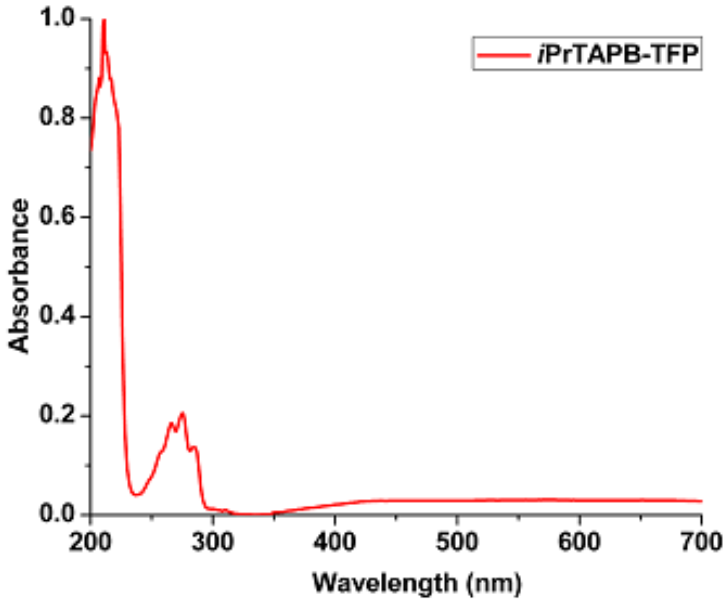

Figure S24. Normalized UV-vis spectrum of *i*PrTAPB-TFP acetonitrile suspension**.**

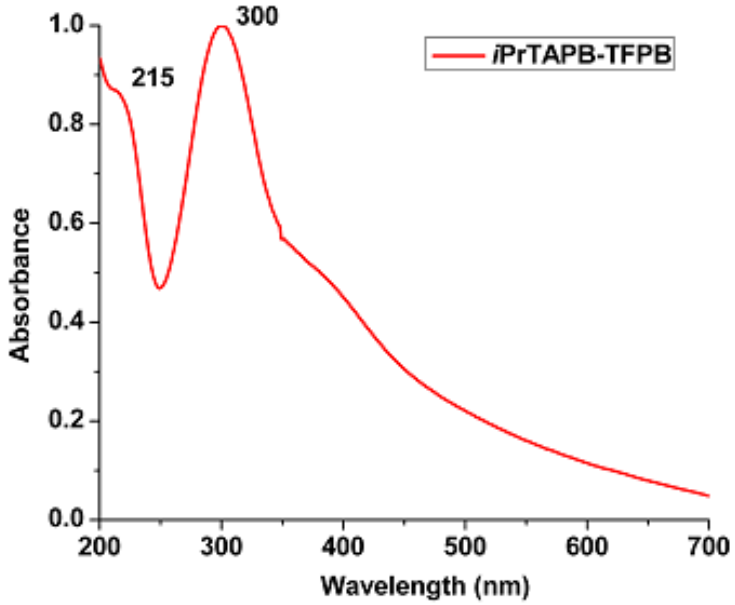

Figure S25. Normalized UV-vis spectrum of *i*PrTAPB-TFPB acetonitrile suspension.

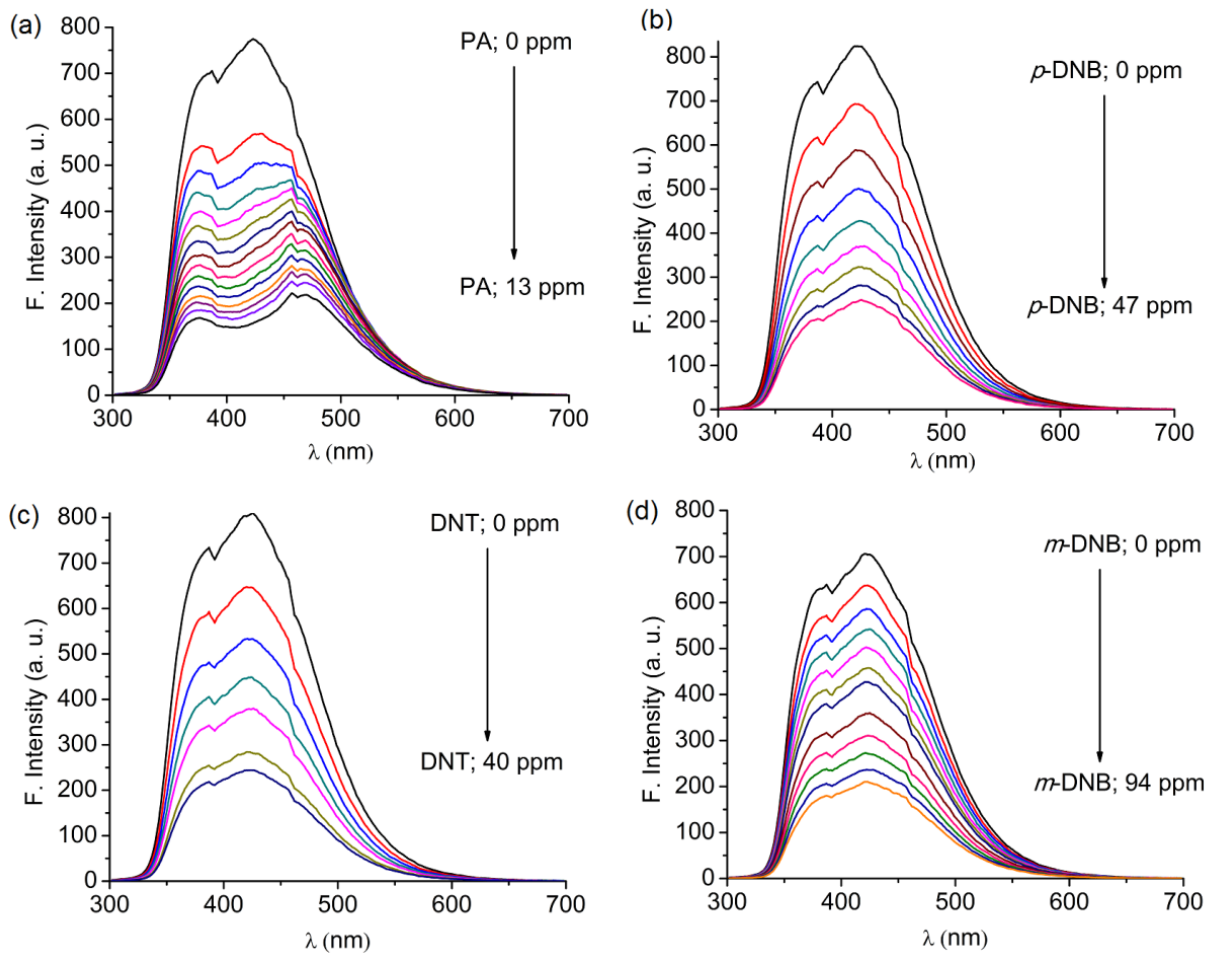

Figure S26. Fluorescence quenching profiles of compound TAPB-TFPB with different PNAC analytes in acetonitrile suspension (λ_{ex} = 285 nm).

Table S2. Details of quenching efficiencies for TAPB-TFPB with different PNAC analytes (13 ppm each).

Analyte(s)	**% Quenching**	**K_{SV} (M^{-1})**
PA	80	5.9×10^4
DNT	36	8.7×10^3
m-DNB	19	3.3×10^3
p-DNB	31	7.6×10^3

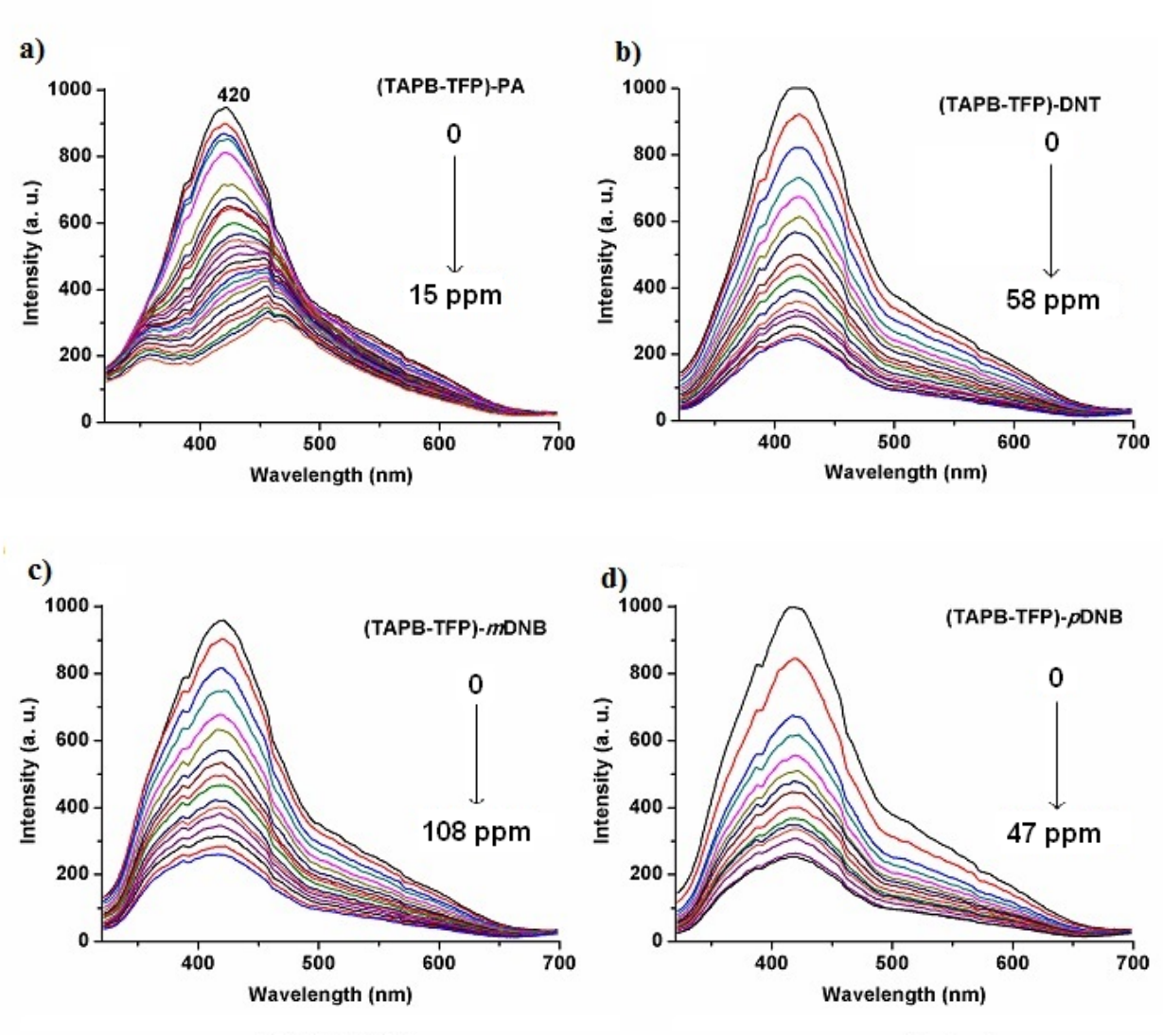

Figure S27. Fluorescence quenching of TAPB-TFP with a) PA; b) DNT; c) *m*DNB; d) *p*DNB (λ_{ex} = 285 nm).

Table S3. Details of quenching efficiencies for TAPB-TFP with different PNAC analytes (15 ppm each).

Analyte(s)	% Quenching	K_{SV} (M^{-1})
PA	67	3.2×10^4
DNT	19	8.7×10^3
m-DNB	10	2.8×10^3
p-DNB	23	9.6×10^3

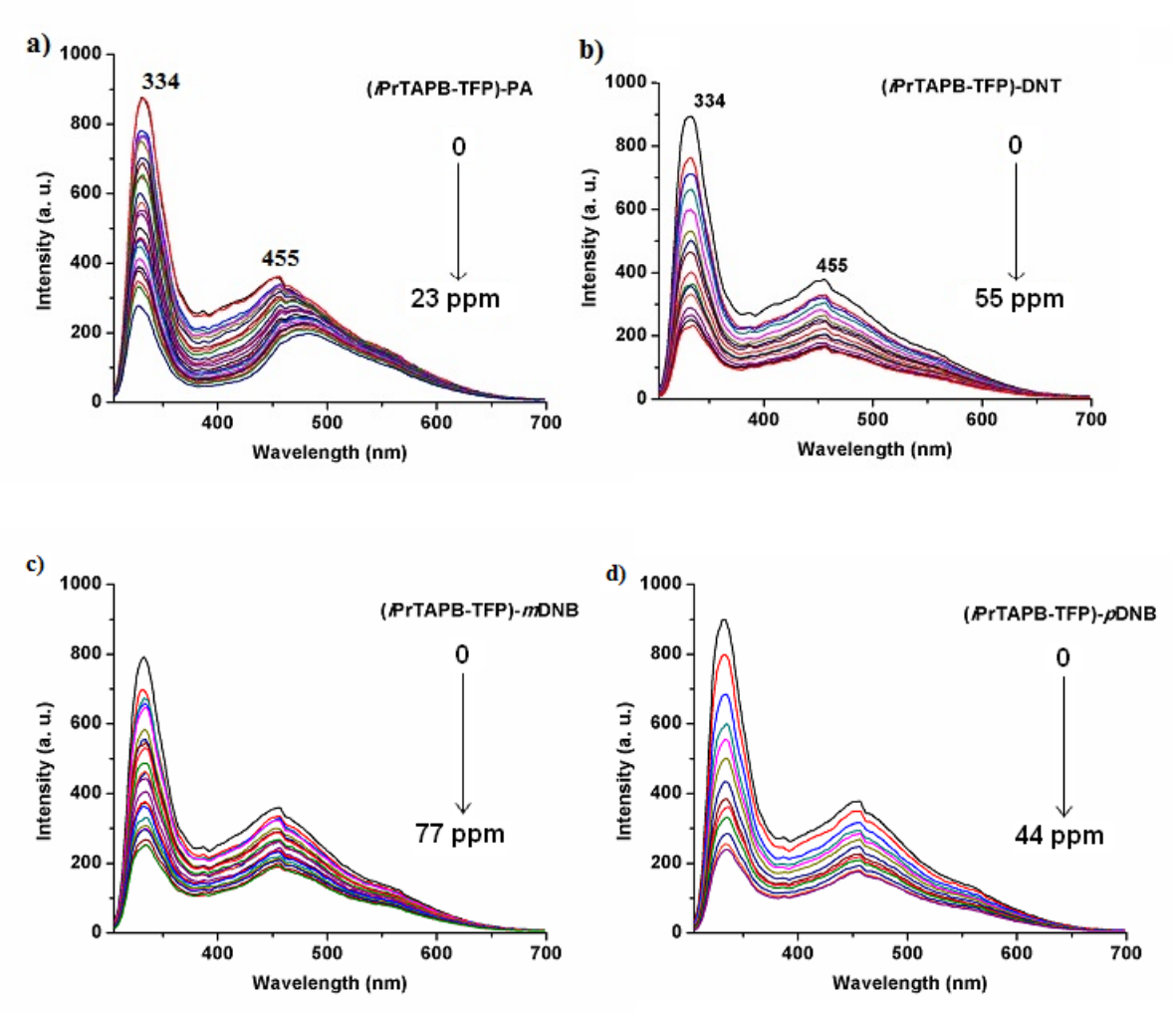

Figure S28. Fluorescence quenching of *i*PrTAPB-TFP with a) PA; b) DNT c) *m*DNB; d) *p*DNB (λ_{ex} = 290 nm).

Table S4. Details of quenching efficiencies for *i*PrTAPB-TFP with different PNAC analytes (23 ppm each).

Analyte(s)	% Quenching	K_{SV} (M^{-1})
PA	68	1.8×10^4
DNT	31	8.8×10^3
m-DNB	20	4.2×10^3
p-DNB	39	1.1×10^4

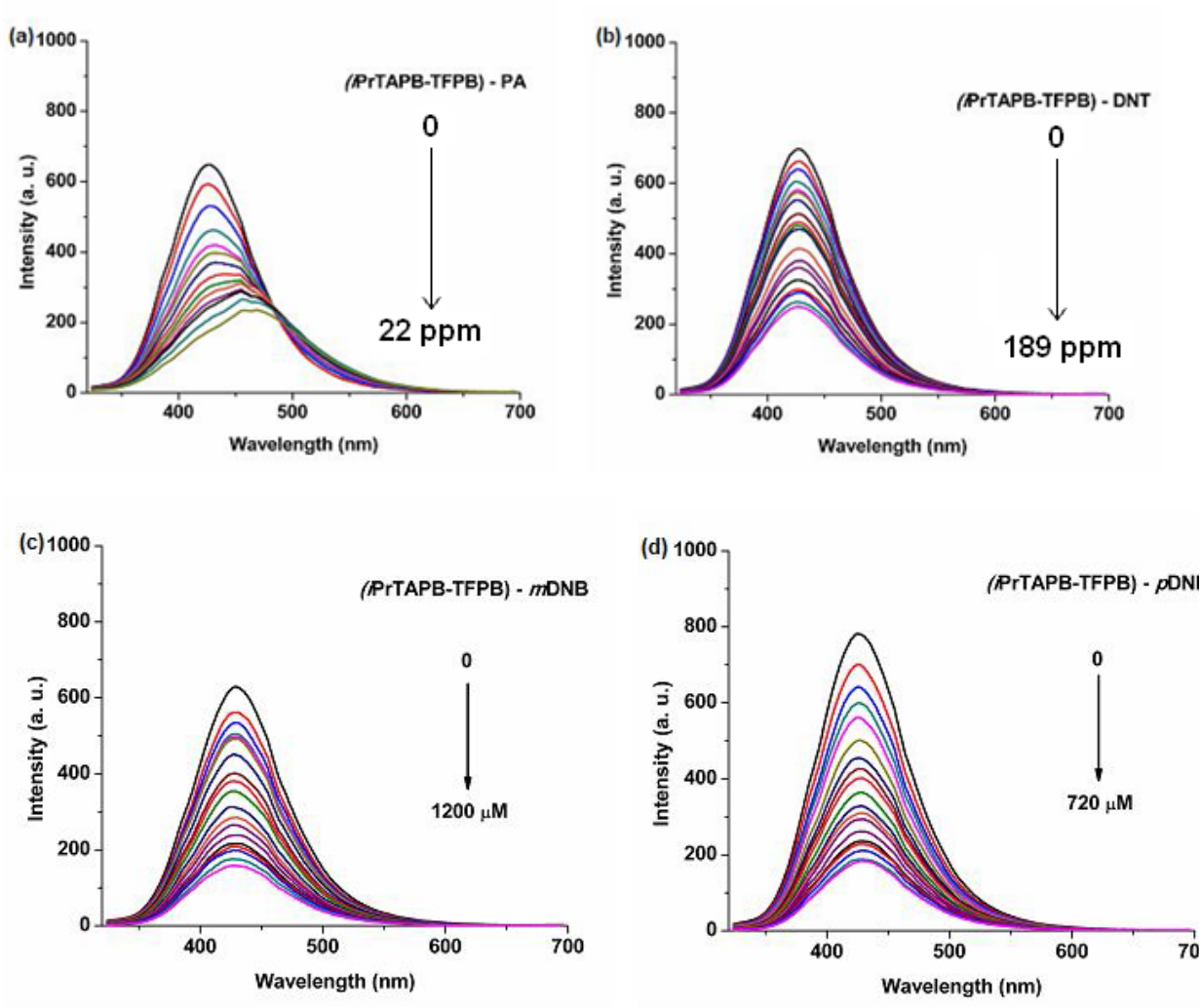

Figure S29. Fluorescence quenching of *i*PrTAPB-TFPB with a) PA; b) DNT c) *m*DNB; d) *p*DNB (λ_{ex} = 300 nm).

Table S5. Details of quenching efficiencies for *i*PrTAPB-TFPB with different PNAC analytes (22 ppm each).

Analyte(s)	% Quenching	K_{SV} (M^{-1})
PA	64	3.0×10^4
DNT	8	1.2×10^3
m-DNB	8	1.7×10^3
p-DNB	14	3.1×10^3

Table S6. Crystallographic information of *i*PrTAPB-NPh_2 and TAPB-Benz

Compound	***i*PrTAPB-NPh_2**	**TAPB-Benz**
Empirical formula	$C_{81}H_{81}N_3$	$C_{94}H_{76}N_6O$
Formula weight	1096.49	1305.61
Temperature (K)	150(2)	100(2)
Wavelength (Å)	0.71075	1.54190
Crystal system	Monoclinic	Monoclinic
Space group	*P* 21/*n*	*P* 21
a (Å)	9.392(4)	7.341(4)
b (Å)	25.613(13)	30.358(14)
c (Å)	32.908(16)	16.214(9)
α (°)	90	90
β (°)	97.3580(10)	97.409(11)
γ (°)	90	90
Volume ($Å^3$)	7851(6)	3583(3)
Z	4	2
Density (calculated) (Mg/m^3)	0.928	1.210
Absorption coefficient (mm^{-1})	0.053	0.549
F(000)	2352	1380
Crystal size (mm^3)	0.20 x 0.20 x 0.20	0.21 x 0.09 x 0.04
Theta range for data collection	2.50 to 25.00°.	6.75 to 59.99°
Reflections collected	58370	15608
Goodness-of-fit on F^2	1.080	1.110
Final R indices [I>2sigma(I)]	R1 = 0.0890, wR2 = 0.2247	R1 = 0.0710, wR2 = 0.1614
R indices (all data)	R1 = 0.1200, wR2 = 0.2476	R1 = 0.1005, wR2 = 0.1891

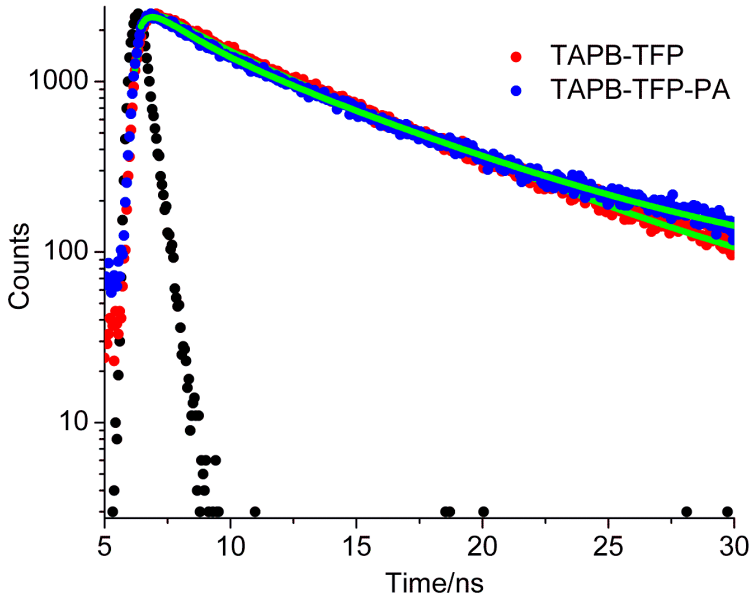

Figure S30. Time resolved fluorescence decays for acetonitrile suspension of TAPB-TFP before (red) and after addition of PA (blue). Biexponential fits to the decays are included as solid lines (green).

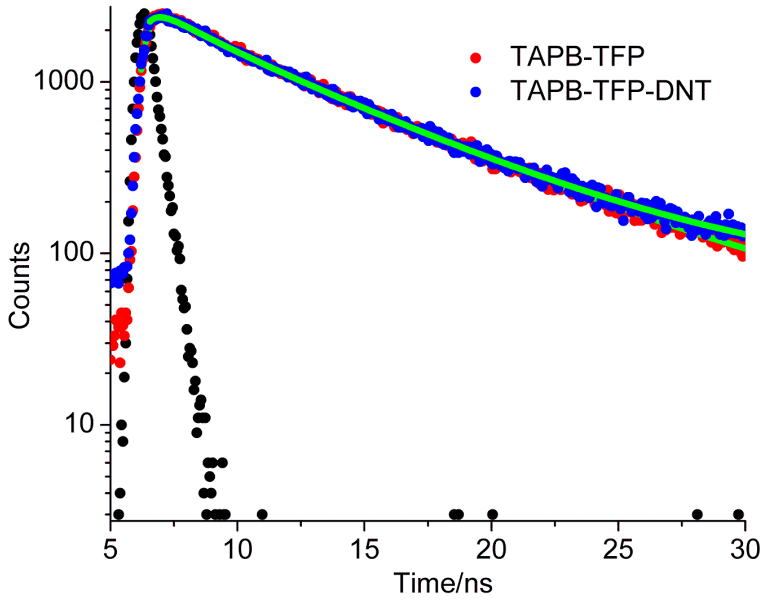

Figure S31. Time resolved fluorescence decays for acetonitrile suspension of TAPB-TFP before (red) and after addition of DNT (blue). Biexponential fits to the decays are included as solid lines (green).

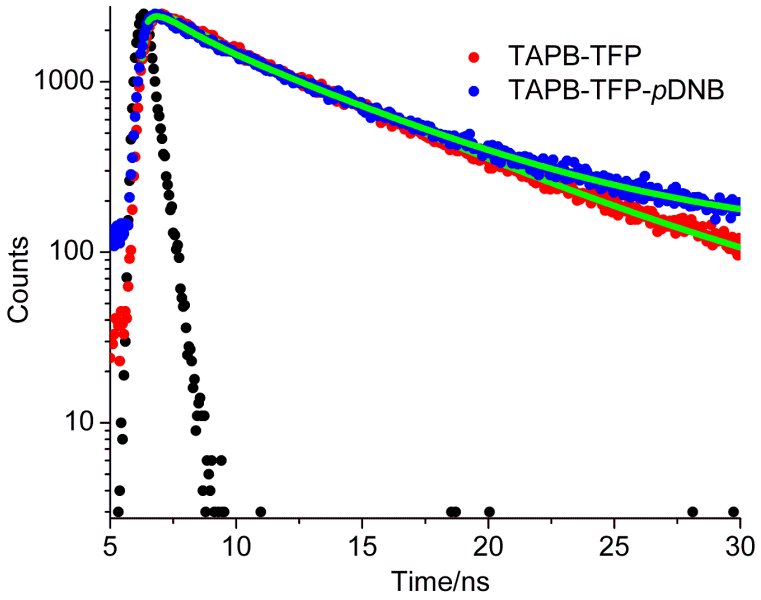

Figure S32. Time resolved fluorescence decays for acetonitrile suspension of TAPB-TFP before (red) and after addition of *p*DNB (blue). Biexponential fits to the decays are included as solid lines (green).

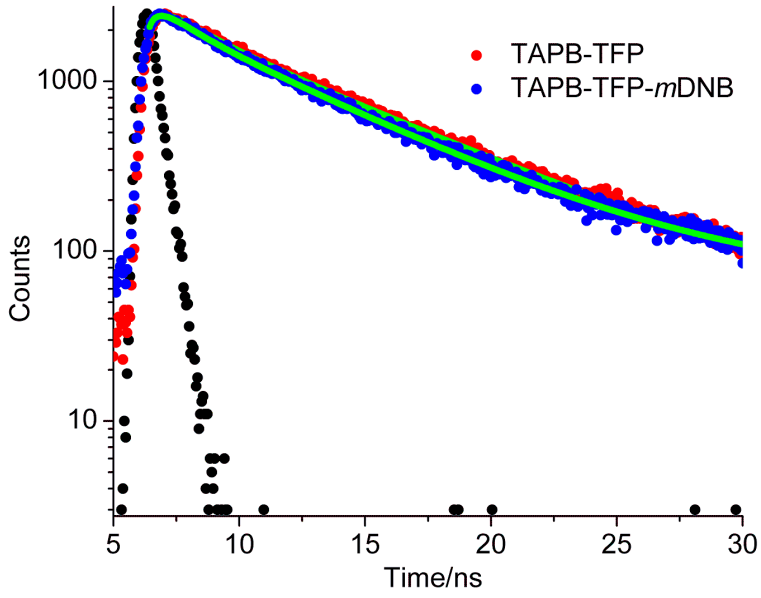

Figure S33. Time resolved fluorescence decays for acetonitrile suspension of TAPB-TFP before (red) and after addition of *m*DNB (blue). Biexponential fits to the decays are included as solid lines (green).

Table S7. Lifetime measurement of the excited state of TAPB-TFP with various polynitroaromatic analytes.

Compounds	Analyte concentration (ppm)	τ_1 (ns)	τ_2 (ns)	χ^2
TAPB-TFP	-	1.7	6.8	1.01
TAPB-TFP-PA	15	1.7	7.0	1.02
TAPB-TFP-DNT	58	2.0	6.4	1.08
TAPB-TFP-*p*DNB	47	1.1	6.5	1.05
TAPB-TFP-*m*DNB	108	1.3	6.0	1.05

References

1. C. Zhang, X. Yang, Y. Zhao, X. Wang, M. Yu and J. –X. Jiang, *Polymer*, 2015, **61**, 36.
2. V. S. P. K. Neti, J. Wang, S. Deng and L. Echegoyen, *RSC Adv.*, 2015, **5**, 10960.
3. A. K. Sekizkardes, T. Islamoglu, Z. Kahveci and H. M. El-Kaderi, *J. Mater. Chem. A*, 2014, **2**, 12492.
4. Z. –Z. Yang, H. Zhang, B. Yu, Y. Zhao, G. Ji and Z. Liu, *Chem. Commun.,* 2015, **51**, 1271.
5. J. Lu and J. Zhang, *J. Mater. Chem. A*, 2014, **2**, 13831.
6. H. A. Patel, D. Ko and C. T. Yavuz, *Chem. Mater.*, 2014, **26**, 6729.
7. B. Ashourirad, A. K. Sekizkardes, S. Altarawneh and H. M. El-Kaderi, *Chem. Mater.*, 2015, **27**, 1349.
8. A. K. Sekizkardes, S. Altarawneh, Z. Kahveci, T. Islamoglu and H. M. El-Kaderi, *Macromolecules*, 2014, **47**, 8328.
9. Z. Chang, D.-S. Zhang, Q. Chen and X.-H. Bu, *Phys. Chem. Chem. Phys.*, 2013, **15**, 5430.
10. R. Dawson, E. Stockel, J. R. Holst, D. J. Adams and A. I. Cooper, *Energy Environ. Sci.*, 2011, **4**, 4239.
11. P. Z. Li and Y. L. Zhao, *Chem.-Asian J.*, 2013, **8**, 1680.

12. Y. Zhu, H. Long and W. Zhang, *Chem. Mater.*, 2013, **25**, 1630.
13. S. Kandambeth, A. Mallick, B. Lukose, M. V. Mane, T. Heine and R. Banerjee, *J. Am. Chem. Soc.*, 2012, **134**, 19524.
14. X. Wang, Y. Zhao, L. Wei, C. Zhang, X. Yang, M. Yu and J.-X. Jiang, *Macromolecular Chemistry and Physics*, 2015, **216**, 504.